The Standard Finite Element Method and the Weak Galerkin Method for Elliptic Boundary Value Problems

Dailin Tang
17marktaylor@gmail.com

Department of Mathematics
Jilin University, Changchun

June 10, 2021

Applications of FEM

Typical area of interest:

- aeronautical industry, e.g. aircraft designing
- automotive industry, e.g. car designing
- civil engineering, e.g. 3D modeling
- biomechanical industry, e.g. medical image
- solving PDEs
- ...

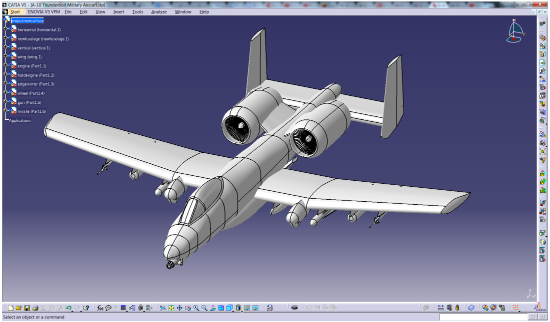
CATIA V5 - [A-10 Thunderbolt Military Aircraft.stp]
Start
ENOVIA V5 VPM
File
Edit
View
Insert
Tools
Analyze
Window
Help
projectnewsurface
horizontal (horizontal.1)
newfuselage (newfuselage.1)
vertical (vertical.1)
wing (wing.1)
engine (Part1.1)
holdengine (Part1.2)
edgemirror (Part1.3)
wheel (Part1.4)
gun (Part1.5)
missile (Part1.6)
Applications
Select an object or a command

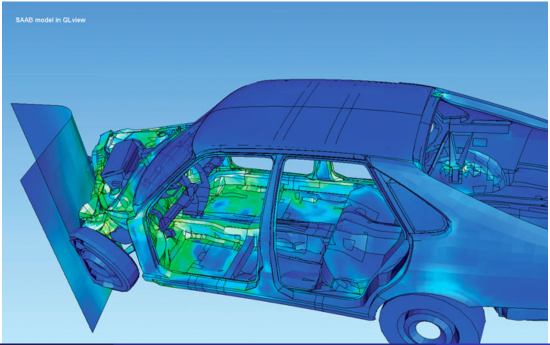
SAAB model in GLview

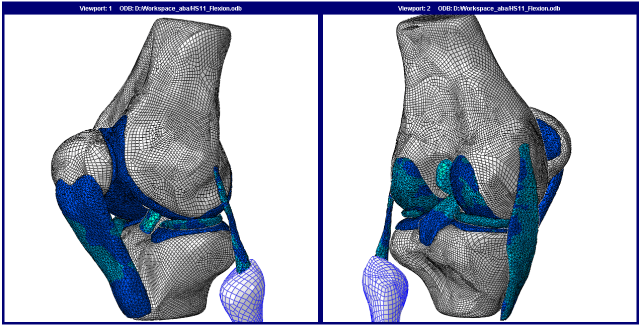

As the computational kernel in game engines

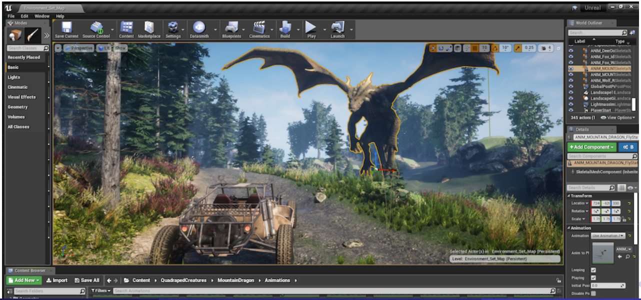

The Model Problems

P1: A one-dimensional two-point boundary value problem with homogeneous Dirichlet boundary conditions

$$-\frac{\mathrm{d}}{\mathrm{d}x}\left(p(x)\frac{\mathrm{d}u}{\mathrm{d}x}\right)+q(x)u=f(x), \quad x\in(a,b), \tag{1}$$

$$u(a)=0,\ u(b)=0, \tag{2}$$

where $p(x)\in C^1(\bar{I}),\ p(x)\geq p_{min}>0,\ q(x)\in C^1(\bar{I}),\ q(x)\geq 0,\ f(x)\in L^2(I),\ I=]a,b[$.

P2: A second-order elliptic homogeneous Neumann problem

$$-\nabla\cdot(\boldsymbol{\alpha}(\boldsymbol{x})\nabla u)+\gamma(\boldsymbol{x})u=f, \quad \text{in } \Omega, \tag{3}$$

$$\boldsymbol{\alpha}(\boldsymbol{x})\nabla u\cdot\boldsymbol{n}=0, \quad \text{on } \partial\Omega, \tag{4}$$

where Ω is an open bounded domain in $\mathbb{R}^2$, ∇u denotes the gradient of the function u, $\boldsymbol{\alpha}$ is a symmetric uniformly positive definite 2×2 matrix-valued function, γ is a scalar-valued function, and $\boldsymbol{n}$ is the outward unit vector normal to the boundary $\partial\Omega$.

But What Is Uniformly Positive Definite?

Definition

A matrix-valued function $\mathbf{A} : \Omega \mapsto \mathbb{R}^{n,n}$, $n \in \mathbb{N}$, is called uniformly positive definite, if

$$\exists \epsilon^- > 0 : \quad \boldsymbol{z}^\top \mathbf{A}(\boldsymbol{x})\boldsymbol{z} \geq \epsilon^- \|\boldsymbol{z}\| \quad \forall \boldsymbol{z} \in \mathbb{R}^n$$

for *almost all* $\boldsymbol{x} \in \Omega$, that is, only with the exception of a set of volume zero.

The Galerkin Scheme

The *weak* form:

$$\begin{cases} \text{Find } u \in U \text{ such that} \\ a(u,v) = \ell(v) \quad \forall v \in V. \end{cases} \tag{5}$$

Here $a : U \times V \mapsto \mathbb{R}$ is a continuous bilinear form and $\ell : V \mapsto \mathbb{R}$ is a continuous linear form, with

$$P1 : a(u,v) = \int_a^b \left(p(x) \frac{\mathrm{d}u}{\mathrm{d}x} \frac{\mathrm{d}v}{\mathrm{d}x} + q(x)uv \right) \mathrm{d}x, \quad \ell(v) = \int_a^b fv \,\mathrm{d}x. \tag{6}$$

$$P2 : a(u,v) = \int_\Omega (\alpha(\boldsymbol{x}) \nabla u \cdot \nabla v + \gamma(\boldsymbol{x}) uv) \,\mathrm{d}\boldsymbol{x}, \quad \ell(v) = \int_\Omega fv \,\mathrm{d}\boldsymbol{x}. \tag{7}$$

$$u_h = \mu_1 b_h^1 + \mu_2 b_h^2 + \ldots + \mu_N b_h^N, \quad \mu_i \in \mathbb{R},$$
$$v_h = \nu_1 b_h^1 + \nu_2 b_h^2 + \ldots + \nu_N b_h^N, \quad \nu_i \in \mathbb{R}.$$

$$u_h \in U_h : \quad a(u_h, v_h) = \ell(v_h) \quad \forall v_h \in U_h.$$

$$\Leftrightarrow \quad \sum_{k=1}^{N} \sum_{j=1}^{N} \mu_k \nu_j a(b_h^k, b_h^j) = \sum_{j=1}^{N} \nu_j \ell(b_h^j) \quad \forall \nu_1, \ldots, \nu_N \in \mathbb{R},$$

$$\Leftrightarrow \quad \sum_{j=1}^{N} \nu_j \left(\sum_{k=1}^{N} \mu_k a(b_h^k, b_h^j) - \ell(b_h^j) \right) = 0 \quad \forall \nu_1, \ldots, \nu_N \in \mathbb{R},$$

$$\Leftrightarrow \quad \sum_{k=1}^{N} \mu_k a(b_h^k, b_h^j) = \ell(b_h^j) \quad \text{for } j = 1, \ldots, N.$$

$$\Leftrightarrow \quad \mathbf{A}\vec{\mu} = \vec{\varphi},$$

$$\mathbf{A} = \left[a(b_h^k, b_h^j) \right]_{j,k=1}^{N} \in \mathbb{R}^{N,N}, \ \vec{\mu} = (\mu_1, \ldots, \mu_N)^\top \in \mathbb{R}^N, \ \vec{\varphi} = \left[\ell(b_h^j) \right]_{j=1}^{N}.$$

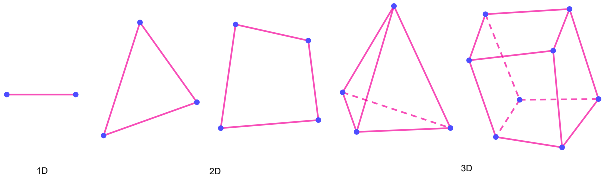

Figure: Types of finite elements

Meshes in 1D: Intervals

Figure: A partition on interval $[a, b]$

Meshes in 2D: Triangulations

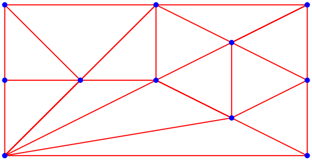

Figure: Triangular mesh in 2D

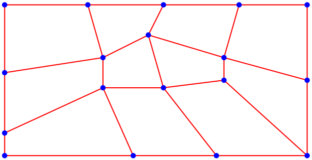

Figure: Quadrilateral mesh in 2D

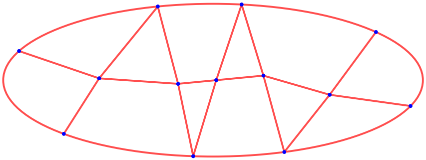

Figure: A 2D *hybrid* mesh comprising triangles, quadrilaterals, and curvilinear cells (at $\partial\Omega$)

Definition (Triangulation)

A triangulation $\mathcal{M}$ of Ω satisfies

1. $\mathcal{M} = \{K_i\}_{i=1}^{M}, \; M \in \mathbb{R}, \; K_i :=$ open triangle
2. disjoint interiors: $i \neq j \Rightarrow K_i \cap K_j = \varnothing$
3. tiling/partition property: $\displaystyle\bigcup_{i=1}^{M} \overline{K}_i = \overline{\Omega}$
4. intersection $\overline{K}_i \cap \overline{K}_j$, $i \neq j$ is
   - either $\varnothing$,
   - or an edge of both triangles,
   - or a vertex of both triangles.

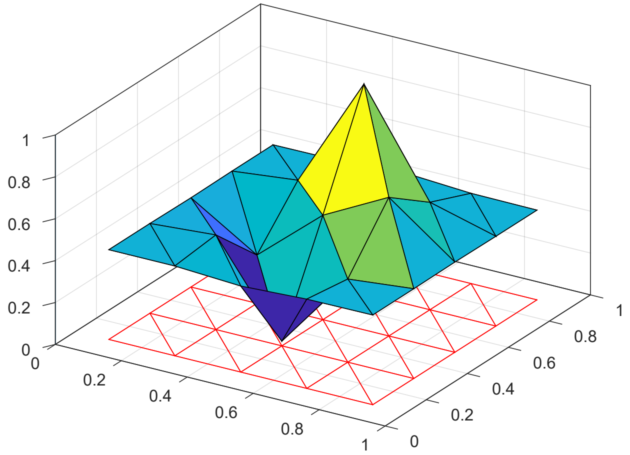

Figure: $\Uparrow$ a continuous piecewise affine linear function $\in \mathcal{S}_1^0(\mathcal{M})$ on a triangular mesh $\mathcal{M}$

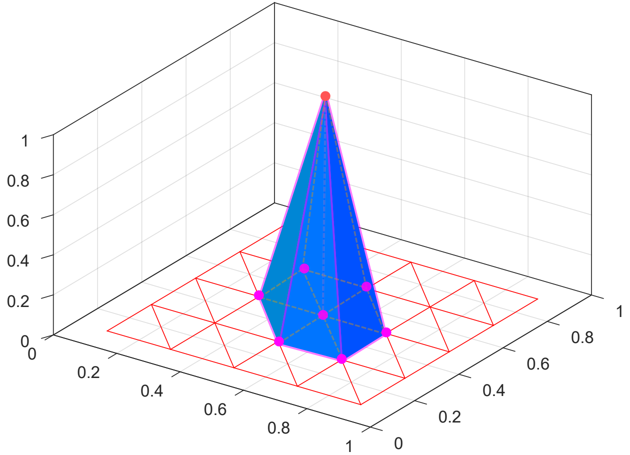

Figure: A (global) piecewise linear nodal basis function on a triangular mesh $\mathcal{M}$

Nodal Basis Functions

$$b_h^j \in \mathcal{S}_1^0(\mathcal{M}),$$

$$b_h^j(\boldsymbol{x}_i) = \begin{cases} 1, & \text{if } \boldsymbol{x}_i = \boldsymbol{x}_j, \\ 0, & \text{if } \boldsymbol{x}_i \in \mathcal{V}(\mathcal{M}) \setminus \{\boldsymbol{x}_j\}, \end{cases}$$

$$i, j = \{1, ..., N\}.$$

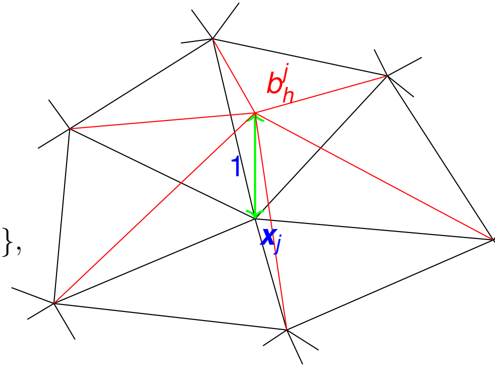

Galerkin Matrices in 1D

$$\int_a^b \frac{\mathrm{d}b_h^j}{\mathrm{d}x}(x)\frac{\mathrm{d}b_h^i}{\mathrm{d}x}(x)\,\mathrm{d}x = \begin{cases} 0, & \text{if } |i-j| > 2, \quad \rightarrow \\ -\dfrac{1}{h_{i+1}}, & \text{if } j = i+1, \quad \rightarrow \\ -\dfrac{1}{h_i}, & \text{if } j = i-1, \quad \rightarrow \\ \dfrac{1}{h_i} + \dfrac{1}{h_{i+1}}, & \text{if } 1 \le i = j \le M-1. \quad \rightarrow \end{cases}$$

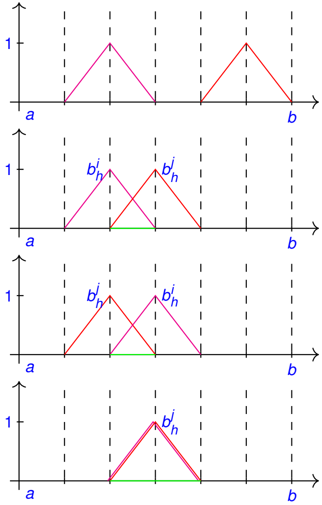

Barycentric Coordinate Functions

Let $\boldsymbol{a}_K^1, \boldsymbol{a}_K^2, \boldsymbol{a}_K^3$ be the vertices of the triangle K with coordinates $\boldsymbol{a}_K^1 = \begin{bmatrix} a_1^1 \\ a_2^1 \end{bmatrix}, \ \boldsymbol{a}_K^2 = \begin{bmatrix} a_1^2 \\ a_2^2 \end{bmatrix}, \text{ and } \boldsymbol{a}_K^3 = \begin{bmatrix} a_1^3 \\ a_2^3 \end{bmatrix}$, we write

$$\lambda_i := b^j_{h|K} \quad \text{with} \quad \boldsymbol{a}_K^i = \boldsymbol{x}_j. \qquad \begin{bmatrix} i \leftrightarrow \textit{local} \text{ vertex number} \\ j \leftrightarrow \textit{global} \text{ node number} \end{bmatrix}$$

Here, $\lambda_1, \lambda_2, \lambda_3$ are the barycentric coordinates functions.

Visual of Barycentric Coordinate Functions

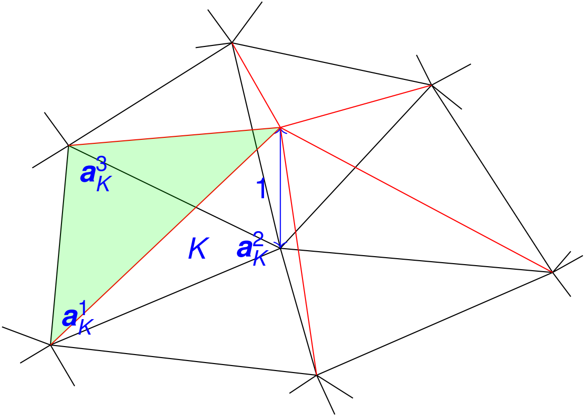

Figure: $\Uparrow$ a barycentric coordinate function λ_2

Element Matrices

$$\mathbf{A}_K := \left[\int_K \mathbf{grad}\, \lambda_i \cdot \mathbf{grad}\, \lambda_j \,\mathrm{d}\boldsymbol{x} \right]_{i,j=1}^{3} \in \mathbb{R}^{3,3} \tag{8}$$

$$\mathbf{A}_K = |K| \begin{bmatrix} \beta_1^1 & \beta_1^2 & \beta_1^3 \\ \beta_2^1 & \beta_2^2 & \beta_2^3 \end{bmatrix}^\top \begin{bmatrix} \beta_1^1 & \beta_1^2 & \beta_1^3 \\ \beta_2^1 & \beta_2^2 & \beta_2^3 \end{bmatrix} \in \mathbb{R}^{3,3}, \tag{9}$$

where $\begin{bmatrix} \beta_1^1 & \beta_1^2 & \beta_1^3 \\ \beta_2^1 & \beta_2^2 & \beta_2^3 \end{bmatrix}$ can be computed by

$$\begin{bmatrix} \beta_1^1 & \beta_1^2 & \beta_1^3 \\ \beta_2^1 & \beta_2^2 & \beta_2^3 \end{bmatrix} = \left(\begin{bmatrix} 1 & a_1^1 & a_2^1 \\ 1 & a_1^2 & a_2^2 \\ 1 & a_1^3 & a_2^3 \end{bmatrix}^{-1} \right)_{(2:3,:)} . \tag{10}$$

Vertex-centered Assembly

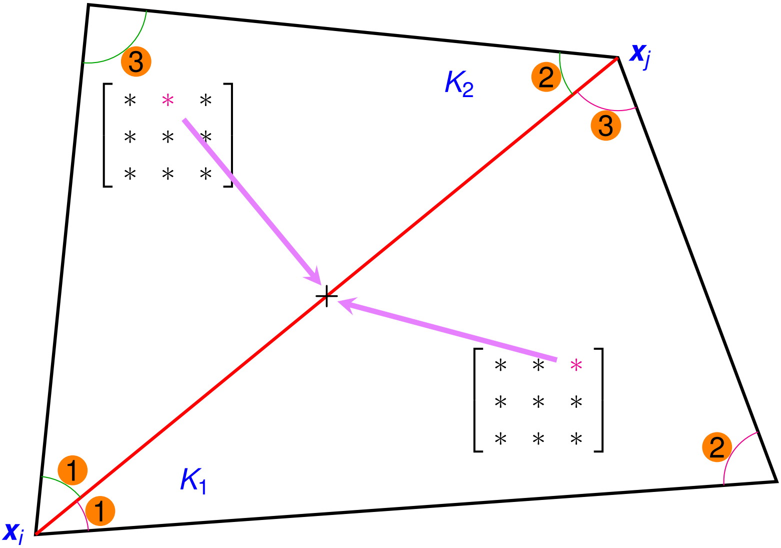

Figure: $\mathbf{A}_{ij}$ by summing entries of two element matrices

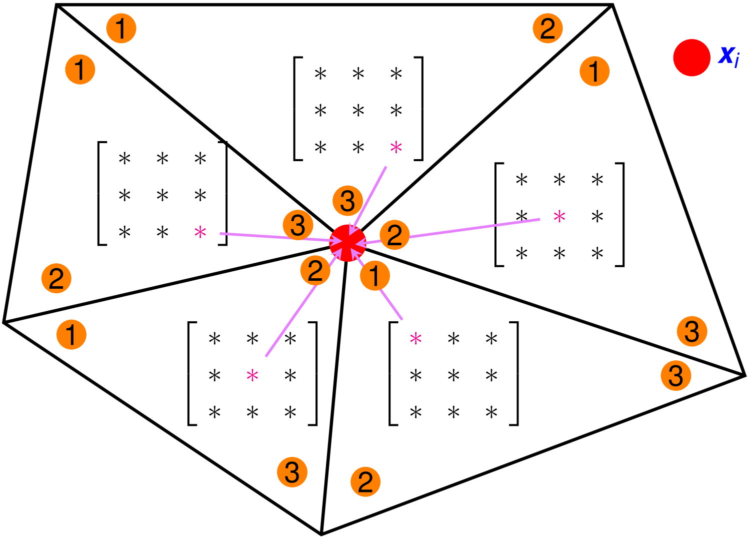

Figure: $\mathbf{A}_{ii}$ by summing diagonal entries of element matrices of adjacent triangles

Vertex-centered Assembly Algorithm

Vertex-centered assembly of Galerkin matrix for linear finite elements

for all $e \in \mathcal{E}(\mathcal{M})$ **do**
    $(i,j) :=$ vertex numbers of endpoints of e
    $(\mathbf{A})_{ij} \leftarrow 0,\ (\mathbf{A})_{ji} \leftarrow 0$
    for all trangle K adjacent to e **do**
        find local numbers $l, m \in \{1,2,3\}$ of endpoints of e
        $(\mathbf{A})_{ij} \leftarrow (\mathbf{A})_{ij} + (\mathbf{A}_K)_{lm}$ ▷ see Figure 9
        $(\mathbf{A})_{ji} \leftarrow (\mathbf{A})_{ji} + (\mathbf{A}_K)_{ml}$ ▷ see Figure 9
    end for
end for
for all $\boldsymbol{v} \in \mathcal{V}(\mathcal{M})$ **do**
    $j :=$ number of vertex $\boldsymbol{v}$
    $(\mathbf{A})_{jj} \leftarrow 0$
    for all trangle K adjacent to $\boldsymbol{v}$ **do**
        $l :=$ local number of e in K
        $(\mathbf{A})_{jj} \leftarrow (\mathbf{A})_{jj} + (\mathbf{A}_K)_{ll}$ ▷ see Figure 10
    end for
end for

Cell-oriented Assembly

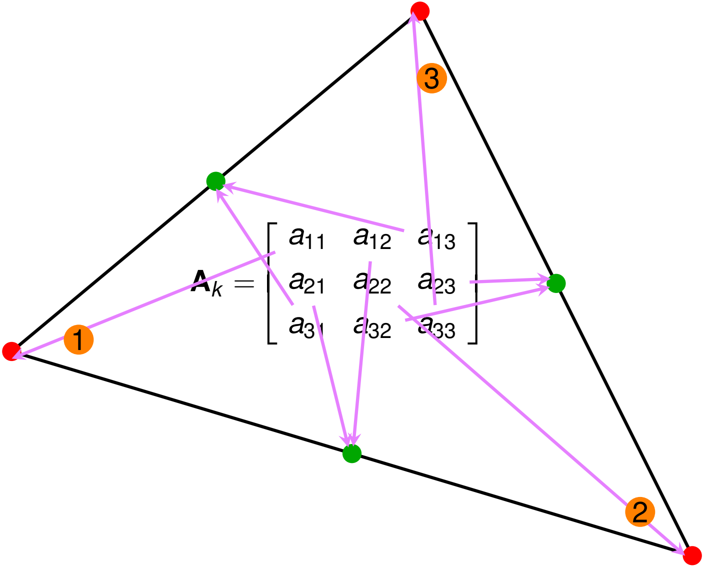

Figure: Cell-oriented assembly of Galerkin matrix by distribution from element

Cell-oriented assembly of Galerkin matrix for linear finite elements

SparseMatrix $\mathbf{A} \in \mathbb{R}^{N,N}, \; N := \sharp\mathcal{V}(\mathcal{M})$
$\mathbf{A} := \mathbf{0}$
$M := \sharp\mathcal{M}$ ▷ no. of cells
for $i = 1$ **to** M **do**
    $K \leftarrow$ `mesh.getElemCoords`(i) ▷ obtain cell-shape information
    $\mathbf{A}_K \leftarrow$ `getElemMatrix`(K) ▷ compute element matrix, see (9, 10)
    for $k = 1$ **to** 3 **do**
        for $j = 1$ **to** 3 **do**
            $\mathbf{A}(i : \boldsymbol{x}^i = \boldsymbol{a}_K^k, \ell : \boldsymbol{x}^\ell = \boldsymbol{a}_K^j) \mathrel{+}= \mathbf{A}_K(k, j)$ ▷ see Figure 11
        end for
    end for
end for

Computation of RHS Vector

$\longrightarrow$

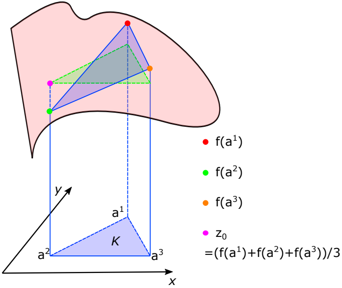

$$\int_K f(\boldsymbol{x})\,\mathrm{d}\boldsymbol{x} \approx \frac{|K|}{3}\left(f(\boldsymbol{a}^1)+f(\boldsymbol{a}^2)+f(\boldsymbol{a}^3)\right)$$

$$\vec{\varphi}_K := [\ell_K(\lambda_i)]_{i=1}^3 \approx \frac{|K|}{3}\begin{bmatrix} f(\boldsymbol{a}^1) \\ f(\boldsymbol{a}^2) \\ f(\boldsymbol{a}^3) \end{bmatrix}$$

Error Estimates

For p-th order finite elements, the error measured in the L^∞-norm is of order $O(h^{p+1})$

$$\|u - u_h\|_{L^\infty(\Omega)} \leq Ch^{p+1}\|u\|,$$

in the L^2-norm is of order $O(h^{p+1})$

$$\|u - u_h\|_{L^2(\Omega)} \leq Ch^{p+1}\|u\|,$$

and in the H^1-norm is of order $O(h^p)$

$$\|u - u_h\|_{H^1(\Omega)} \leq Ch^p\|u\|.$$

DOF Mapper

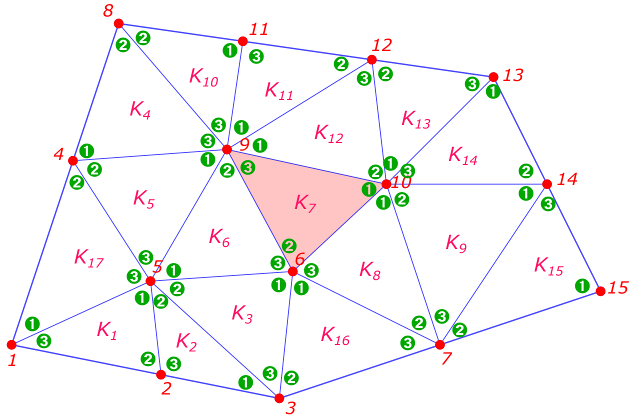

$\sharp$	1	2	3
K_1	5	2	1
K_2	3	5	2
K_3	6	5	3
K_4	4	8	9
K_5	9	4	5
K_6	5	9	6
K_7	10	6	9
K_8	10	7	6
K_9	14	10	7
K_{10}	11	8	9
K_{11}	9	12	11
K_{12}	9	10	12
K_{13}	10	12	13
K_{14}	13	14	10
K_{15}	15	7	14
K_{16}	6	3	7
K_{17}	1	4	5

Mesh Refinement

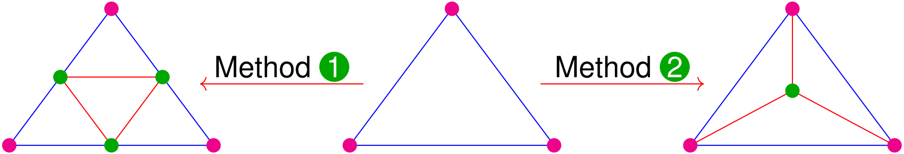

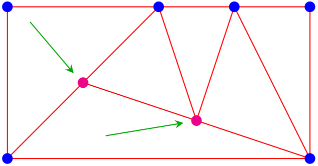

Note: avoid “hanging nodes", each triangle side should be entirely shared by two adjacent triangles

Incorporation of Boundary Conditions

Consider the non-homogeneous Dirichlet boundary value problem

$$-\nabla \cdot (\alpha(\boldsymbol{x})\nabla u) + \gamma(\boldsymbol{x})u = f, \quad \text{in } \Omega, \tag{11}$$

$$u = g_d, \quad \text{on } \partial\Omega, \tag{12}$$

with variational formulation

$$\begin{matrix} u \in H^1(\Omega) \\ u = g_d \text{ on } \partial\Omega \end{matrix} : \int_\Omega (\alpha(\boldsymbol{x})\nabla u \cdot \nabla v + \gamma(\boldsymbol{x})uv)\,\mathrm{d}\boldsymbol{x} = \int_\Omega fv\,\mathrm{d}\boldsymbol{x} \quad \forall v \in H_0^1(\Omega \tag{13}$$

Incorporation of Boundary Conditions

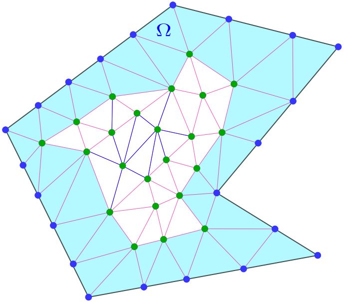

"Location" of nodal basis functions:

$\bullet$, $\bullet$ $\rightarrow$ nodal basis functions of $\mathcal{S}_1^0(\mathcal{M})$

$\bullet$ $\rightarrow$ nodal basis functions of $\mathcal{S}_{1,0}^0(\mathcal{M})$

■ $\rightarrow$ maximum support of offset function u_0:

$$\operatorname{supp}(u_0) \subset \bigcup \{K \in \mathcal{M} : \overline{K} \cap \partial\Omega \neq \emptyset\}.$$

Incorporation of Boundary Conditions

$$\begin{aligned}\mathfrak{B}_0 &:= \{b_h^1, \dots, b_h^{N_0}\} &&\hat{=} \quad \text{nodal basis of } \mathcal{S}_{1,0}^0(\mathcal{M}) \\ \mathfrak{B} &:= \mathfrak{B}_0 \cup \{b_h^{N_0+1}, \dots, b_h^{N}\} &&\hat{=} \quad \text{nodal basis of } \mathcal{S}_{1}^0(\mathcal{M})\end{aligned}$$

$$\mathbf{A} = \begin{bmatrix} \mathbf{A}_0 & \mathbf{A}_{0\partial} \\ \mathbf{A}_{0\partial}^\top & \mathbf{A}_{\partial\partial} \end{bmatrix}, \qquad \begin{aligned}\mathbf{A}_{0\partial} &:= \left(a(b_h^j, b_h^i)\right)_{\substack{i=1,\dots,N \\ j=N_0+1,\dots,N}} \in \mathbb{R}^{N_0, N-N_0}, \\ \mathbf{A}_{\partial\partial} &:= \left(a(b_h^j, b_h^i)\right)_{\substack{i=N_0+1,\dots,N \\ j=N_0+1,\dots,N}} \in \mathbb{R}^{N-N_0, N-N_0}.\end{aligned}$$

$$\longrightarrow \begin{bmatrix} \mathbf{A}_0 & \mathbf{A}_{0\partial} \\ \mathbf{0} & \mathbf{I} \end{bmatrix} \begin{bmatrix} \vec{\mu}_0 \\ \vec{\mu}_\partial \end{bmatrix} = \begin{bmatrix} \vec{\varphi}_0 \\ \vec{\gamma} \end{bmatrix}. \tag{14}$$

Consideration for Higher Order Elements

The interpolation nodes are comprised of the interior nodes and midpoints, i.e.

$$\mathcal{N} := \mathcal{V}_I(\mathcal{M}) \cup \{\text{midpoints of intervals}\}.$$

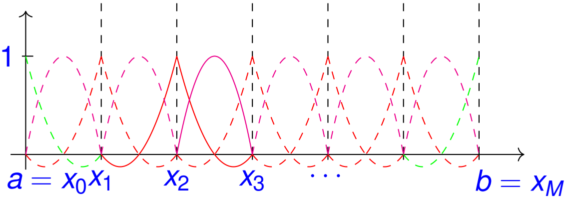

$$u_h = \sum_{i=1}^{M-1} \mu_i b_h^i + \sum_{i=0}^{M-1} \mu_{i+\frac{1}{2}} b_h^{i+\frac{1}{2}},$$

Reference Shape Functions

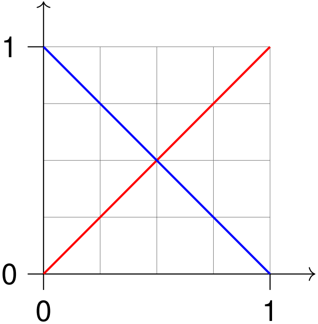

$b^1_{\widehat{K}} = \xi$

$b^2_{\widehat{K}} = 1 - \xi$

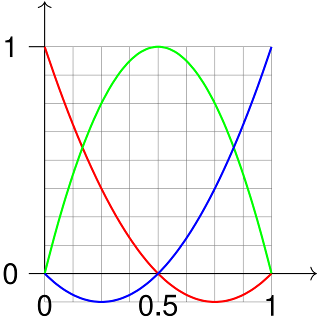

Assembly of Quadratic FE Galerkin Matrix

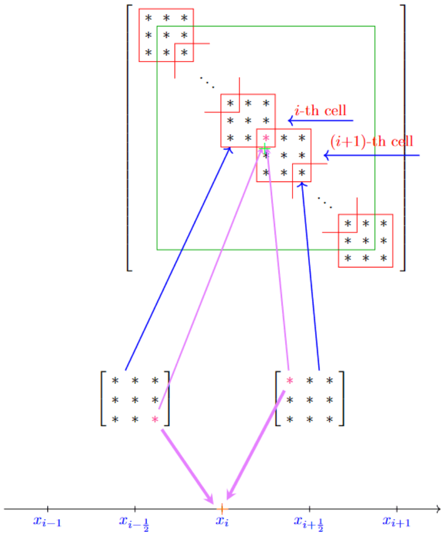

Example 1

Consider the mixed Neumann-Dirichlet BVP

$$
\begin{aligned}
-\Delta u &= 2\pi^2 \cos(\pi x)\cos(\pi y), && \text{in } \Omega \\
\nabla u \cdot \boldsymbol{n} &= \pi \sin(\pi x)\cos(\pi y), && \text{on } \Gamma \\
u &= \cos(\pi x)\cos(\pi y), && \text{on } \partial\Omega \setminus \Gamma,
\end{aligned}
$$

where $\Omega = \{(x,y) \,|\, -\frac{1}{2} < x < 1,\ -1 < y < 1\}$, $\Gamma = \{(x,y) \,|\, x = -\frac{1}{2},\ -1 \le y \le 1\}$.

Example 1

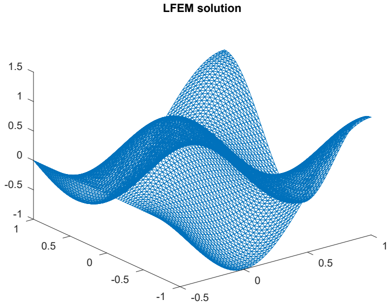
LFEM solution
1.5
1
0.5
0
-0.5
-1
1
0.5
0
-0.5
-1
-0.5
0
0.5
1

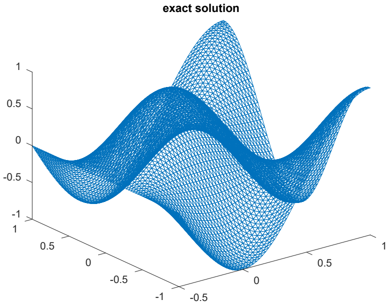
exact solution
1
0.5
0
-0.5
-1
1
0.5
0
-0.5
-1
-0.5
0
0.5
1

Example 1

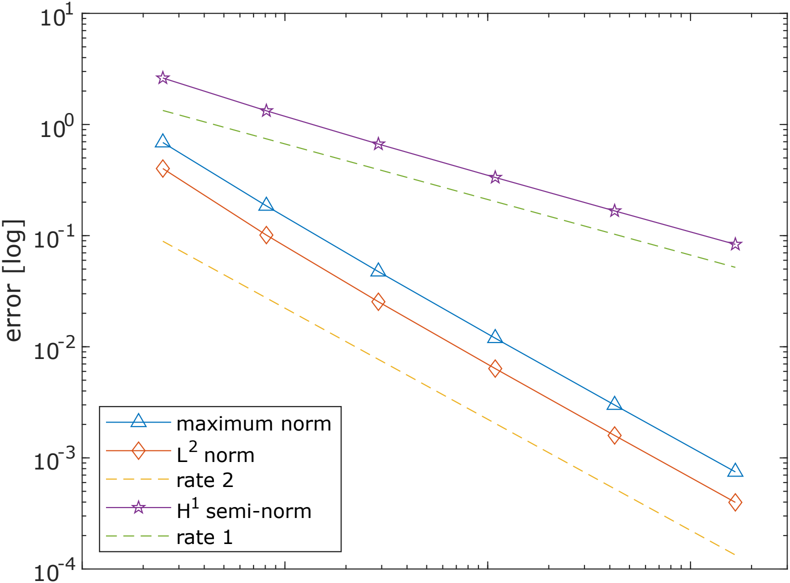

error [log]
10^1
10^0
10^{-1}
10^{-2}
10^{-3}
10^{-4}
maximum norm
L^2 norm
rate 2
H^1 semi-norm
rate 1

Example 3

Consider mixed boundary TPBVP

$$-\frac{\mathrm{d}}{\mathrm{d}x}\left(p(x)\frac{\mathrm{d}u}{\mathrm{d}x}\right)+q(x)u=f(x),\quad x\in(a,b),$$
$$u(a)=0,\ u'(b)=0,$$

where $p(x)\in C^1(\bar{I}),\ p(x)\geq p_{min}>0,\ q(x)\in C^1(\bar{I}),\ q(x)\geq 0,\ f(x)\in L^2(I),\ I=]a,b[$.

Basis Functions for Example 3

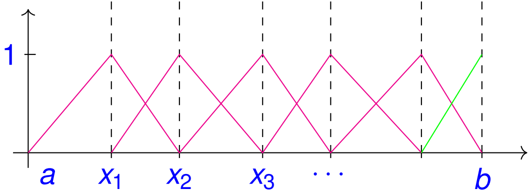

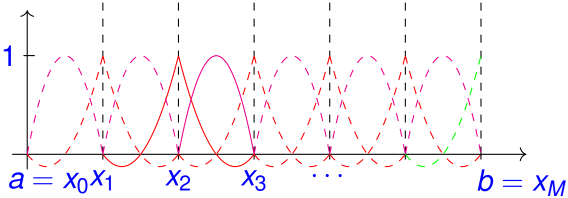

Approximations for Example 3

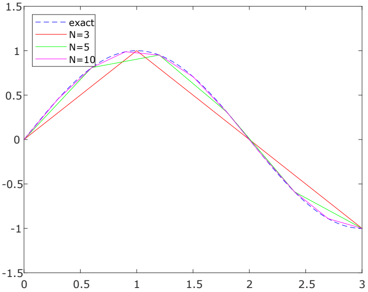

(a) By LFEM

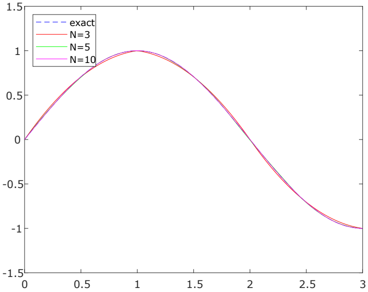

(b) By QFEM

Convergence rates for Example 3

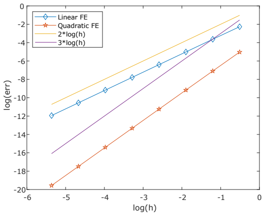

(c) In L^∞ norm

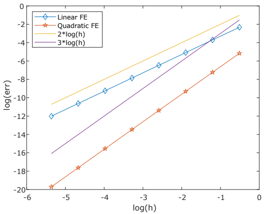

(d) In L^2 norm

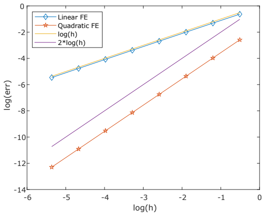

(e) In H^1 norm

WG Model Problem

The Dirichlet problem for 2nd-order elliptic equations

$$-\nabla \cdot (\mathcal{A}\nabla u) = f, \quad \text{in } \Omega, \tag{15}$$

$$u = g, \quad \text{on } \partial\Omega, \tag{16}$$

where Ω is an open bounded domain in $\mathbb{R}^d$ (polygonal for $d = 2$, polyhedral for $d = 3$) and $\mathcal{A}$ is a symmetric uniformly positive definite $d \times d$ matrix-valued function.

Weak Gradients

Weak functions: $v = \{v_0, v_b\}$ satisfying $v_0 \in L^2(T)$ and $v_b \in L^2(\partial T)$
The space of weak functions:

$$W(T) = \{v = \{v_0, v_b\} : \ v_0 \in L^2(T), \ v_b \in L^2(\partial T)\}.$$

Definition

$\forall v \in W(T)$, we define the weak gradient of v as a linear functional $\nabla_w v$ in the dual space of $H^1(T)$ whose action on each $q \in [H^1(T)]^d$ is given by

$$\langle \nabla_w v, q\rangle_T := -(v_0, \nabla \cdot q)_T + \langle v_b, q \cdot \boldsymbol{n}\rangle_{\partial T}. \tag{17}$$

Here, $\boldsymbol{n}$ is the outward normal direction to ∂T.

Definition

The discrete weak gradient operator, denoted by $\nabla_{w,r,T}$, is defined as the unique polynomial $(\nabla_{w,r,T} v) \in [P_r(T)]^d$ satisfying

$$(\nabla_{w,r,T} v, q)_T := -(v_0, \nabla \cdot q) + \langle v_b, q \cdot \boldsymbol{n}\rangle_{\partial T}, \quad q \in [P_r(T)]^d. \tag{18}$$

Remark

We point out that in the design of numerical methods for partial differential equations, the classical gradient operator $\nabla = (\partial_{x_1}, \partial_{x_2})$ should be employed to functions with some certain degree of smoothness. For instance, in the standard Galerkin FEM, continuous piecewise polynomials over a prescribed finite element partition is often implied on such a “smoothness". By introducing the weak gradient operator, derivatives can be taken for functions *without any continuity* across cells on a mesh (amazing). In this way, the notion of weak gradient *permits the use of generalized functions* in approximation.

$\Downarrow$ leads to

Visual of WG Linear Basis Functions

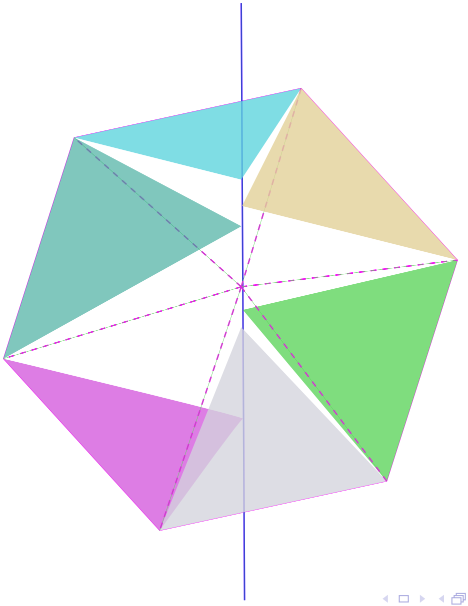

WG Formulation

Find $u_h = \{u_0, u_b\} \in V_h$ such that

$$a(v, w) + s(v, w) = (f, v_0) \quad \forall v \in V_h. \tag{19}$$

Here,

$$a(v, w) = \sum_{T \in \mathcal{T}_h} (a\nabla_w v, \nabla_w w)_T,$$

$$s(v, w) = \rho \sum_{T \in \mathcal{T}_h} h_T^{-1} \langle Q_b v_0 - v_b, Q_b w_0 - w_b \rangle_{\partial T},$$

with $\rho > 0$.

Remark

If we drop the stabilizer $s(\cdot, \cdot)$ and use the classical strong gradient operator ∇ instead of the weak gradient operator ∇_w, then we obtain the standard FEM scheme.

Error Estimates and Convergence

Error Estimates and Convergence

Let $u_h \in V_h$ be the weak Galerkin finite element solution of the model problem (15, 16) arising from (19). Assume the exact solution $u \in H^{k+1}(\Omega)$. Then, there exists a constant C such that

$$\|u_h - Q_h u\| \leq Ch^k \|u\|_{k+1},$$

Moreover, if the usual H^2-regularity is assumed, then

$$\|u - u_0\| \leq Ch^{k+1} \|u\|_{k+1}.$$

❶ Comparison Example 1

$$\mathcal{A} = \begin{bmatrix} x^2+y^2+1 & xy \\ xy & x^2+y^2+1 \end{bmatrix}, \quad \text{with } u = \sin(\pi x)\cos(\pi y).$$

Thus,

$$\begin{aligned} f = & -\pi[3x\cos(\pi x)\cos(\pi y) - 2\pi xy\cos(\pi x)\sin(\pi y) - \\ & 2\pi(x^2+y^2+1)\sin(\pi x)\cos(\pi y) - 3y\sin(\pi x)\sin(\pi y)], \end{aligned}$$

and

$$g = \begin{cases} 0, & x = 0 \text{ or } 1,\ 0 \le y \le 1, \\ sin(\pi x) & y = 0,\ 0 \le x \le 1, \\ -sin(\pi x) & y = 1,\ 0 \le x \le 1, \end{cases} .$$

Numerical Results for Comparison Example 1

Table: Comparison example 1 by WG

h	$\|\|\|e_h\|\|\|$	Order	$\|\|e_0\|\|$	Order
1/4	1.3240e+00		1.5784e+00	
1/8	6.6333e-01	9.9710e-01	3.6890e-01	2.0972
1/16	3.3182e-01	9.9933e-01	9.0622e-02	2.0253
1/32	1.6593e-01	9.9983e-01	2.2556e-02	2.0064
1/64	8.2966e-02	9.9998e-01	5.6326e-03	2.0016
1/128	4.1483e-02	1.0000	1.4078e-03	2.0004

Table: Comparison example 1 by standard FEM

$h_{\mathcal{M}} := n^{-1}$	$\|\|e_u\|\|_\infty$	order	$\|\|e_u\|\|_{L^2(\Omega)}$	order	$\|e_u\|_{H^1(\Omega)}$	order	$\|\|e_u\|\|_{H^1(\Omega)}$	order
1/4	0.0293		0.0644		0.8442		0.8466	
1/8	0.0081	1.8620	0.0176	1.8739	0.4325	0.9648	0.4329	0.9678
1/16	0.0021	1.9284	0.0045	1.9657	0.2176	0.9908	0.2177	0.9917
1/32	0.0005	1.9868	0.0011	1.9912	0.1090	0.9977	0.1090	0.9979
1/64	0.0001	1.9978	0.0003	1.9978	0.0545	0.9994	0.0545	0.9995
1/128	0.0000	1.9989	0.0001	1.9994	0.0273	0.9999	0.0273	0.9999
$O(h^r), r =$		1.9599		1.9713		0.9921		0.9928

Comparison Example 2

❷ Comparison Example 2:
Consider the Poisson problem

$$-\Delta u = f$$

Still, we use the exact solution $u = \sin(\pi x)\cos(\pi y)$ as the first example did. Hence the source function f becomes

$$f = 2\pi^2 \sin(\pi x)\cos(\pi y)$$

and boundary function g is given as before.

Table: Comparison example 2 by WG

h	$\|\|\|e_h\|\|\|$	$\|\|e_h\|\|$	$\|\|e_h\|\|_{\mathcal{E}_h}$
1/2	2.7935e-01	6.1268e-01	5.7099e-02
1/4	1.4354e-01	1.5876e-01	1.3892e-02
1/8	7.2436e-02	4.0043e-02	3.5430e-03
1/16	3.6315e-02	1.0033e-02	8.9325e-04
1/32	1.8170e-02	2.5095e-03	2.2384e-04
1/64	9.0865e-03	6.2747e-04	5.5994e-05
1/128	4.5435e-03	1.5687e-04	1.4001e-05
1/256	2.2718e-03	3.9219e-05	3.5003e-06
$O(h^r)$, $r =$	9.9388e-01	1.9931	1.9961

Table: Comparison example 2 by SG

$h_{\mathcal{M}} := n^{-1}$	$\|\|e_u\|\|_\infty$	order	$\|\|e_u\|\|_{L^2(\Omega)}$	order	$\|e_u\|_{H^1(\Omega)}$	order	$\|\|e_u\|\|_{H^1(\Omega)}$	order
1/4	0.0223		0.0636		0.8440		0.8464	
1/8	0.0059	1.9235	0.0172	1.8863	0.4325	0.9646	0.4328	0.9676
1/16	0.0015	1.9525	0.0044	1.9699	0.2176	0.9908	0.2177	0.9916
1/32	0.0004	1.9752	0.0011	1.9924	0.1090	0.9977	0.1090	0.9979
1/64	0.0001	1.9988	0.0003	1.9981	0.0545	0.9994	0.0545	0.9995
1/128	0.0000	1.9992	0.0001	1.9995	0.0273	0.9999	0.0273	0.9999
$O(h^r)$, $r =$		1.9714		1.9744		0.9921		0.9928

3 Comparison Example 3:
Consider

$$\begin{aligned} -\nabla\cdot(xy\nabla u) &= f, \quad \text{in } \Omega \\ u &= 0. \quad \text{on } \partial\Omega \end{aligned}$$

The exact solution is set to be $u = x(1-x)y(1-y)$ given that it vanishes on the boundary.
The interesting thing is the diffusion tensor $\mathcal{A} = xy$ is not uniformly positive definite (see the 2nd footnote on page 2), that is, we can't find such a positive number $\epsilon^- > 0$ such that

$$((xy)(z))\cdot \boldsymbol{z} \geq \epsilon^- \|\boldsymbol{z}\|^2 \quad \forall \boldsymbol{z} \in \mathbb{R}^2$$

holds for almost all $(x, y) \in \Omega =]0,1[\times]0,1]$. Hence, the convergence rates in these norms by which we have usually measured are not specified. This applies both to WG and SG. So we cannot expect the orders of the convergent rates.

Numerical Results for Comparison Example 3

Table: Comparison example 3 by WG

h	$\|\nabla_d e_h\|$	$\|e_0\|$	$\|e_b\|$	$\|\nabla_d u_h \nabla u\|$	$\|u_0 - u\|$	$\|e_0\|_\infty$
1/8	5.61e-02	3.32e-03	6.60e-03	5.75e-02	5.48e-03	1.27e-02
1/16	4.03e-02	1.38e-03	2.81e-03	4.09e-02	2.59e-03	4.90e-03
1/32	2.95e-02	5.68e-04	1.16e-03	2.96e-02	1.23e-03	2.21e-03
1/64	2.15e-02	2.35e-04	4.83e-04	2.15e-02	5.97e-04	1.16e-03
1/128	1.55e-02	9.93e-05	2.02e-04	1.55e-02	2.91e-04	5.99e-04
$O(h^r)$, $r =$	0.4614	1.2687	1.2594	0.4697	1.0579	1.0912

Table: Comparison example 3 by SG

$h_{\mathcal{M}} := n^{-1}$	$\|e_u\|_\infty$	order	$\|e_u\|_{L^2(\Omega)}$	order	$\|e_u\|_{H^1(\Omega)}$	order	$\|e_u\|_{H^1(\Omega)}$	order
1/4	0.0043		0.0056		0.0590		0.0593	
1/8	0.0019	1.1499	0.0015	1.8432	0.0304	0.9557	0.0305	0.9602
1/16	0.0008	1.3176	0.0004	1.8922	0.0153	0.9909	0.0153	0.9922
1/32	0.0003	1.5415	0.0001	1.9172	0.0076	1.0011	0.0076	1.0015
1/64	0.0001	1.6451	0.0000	1.9340	0.0038	1.0028	0.0038	1.0029
1/128	0.0000	1.6871	0.0000	1.9460	0.0019	1.0022	0.0019	1.0022
$O(h^r)$, $r =$		1.4789		1.9089		0.9928		0.9939

Convergence Rates Unspecified

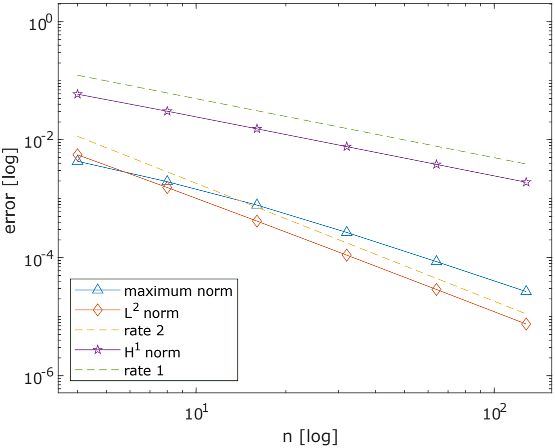

Figure: Comparison example 3 by SG

4. Comparison Example 4:
Consider the anisotropic problem

$$-\nabla \cdot (\mathcal{A}\nabla u) = f,$$

with the diffusion tensor

$$\mathcal{A} = \begin{bmatrix} k^2 & 0 \\ 0 & 1 \end{bmatrix} \quad \text{for } k \neq 0.$$

We set the analytic solution $u = \sin(2\pi x)\sin(2k\pi y)$. Thus the source function

$$f = 8k^2\pi^2 \sin(2\pi x)\sin(2k\pi y)$$

and Dirichlet boundary function

$$g = 0 \quad \text{on } \partial\Omega.$$

We will test two cases with $k = 3$ and $k = 9$ by WG and SG.

Numerical Results for Comp Ex 4 with $k = 3$

Table: Comparison example 4 with $k = 3$ by WG

h	$\|\nabla_d e_h\|$	$\|e_0\|$	$\|e_b\|$	$\|\nabla_d u_h \nabla u\|$	$\|u_0 - u\|$	$\|e_0\|_\infty$
1/8	1.48e+00	1.95e-02	4.61e-02	2.70e+00	1.29e-01	4.13e-02
1/16	7.39e-01	5.11e-03	1.16e-02	1.35e+00	6.53e-02	1.06e-02
1/32	3.69e-01	1.29e-03	2.92e-03	6.80e-01	3.27e-02	2.67e-03
1/64	1.84e-01	3.24e-04	7.33e-04	3.40e-01	1.63e-02	6.68e-04
1/128	9.23e-02	8.12e-05	1.83e-04	1.70e-01	8.18e-03	1.66e-04
$O(h^r)$, $r =$	0.0010	1.9793	1.9942	0.9972	0.9975	1.9906

Table: Comparison example 4 with $k = 3$ by SG

$h_{\mathcal{M}} := n^{-1}$	$\|e_u\|_\infty$	order	$\|e_u\|_{L^2(\Omega)}$	order	$\|e_u\|_{H^1(\Omega)}$	order	$\|e_u\|_{H^1(\Omega)}$	order
1/4	0.6727		0.4879		9.7186		9.7308	
1/8	0.2425	1.4719	0.2875	0.7629	6.8684	0.5008	6.8745	0.5013
1/16	0.0648	1.9050	0.0946	1.6046	3.7577	0.8701	3.7589	0.8709
1/32	0.0180	1.8447	0.0254	1.8967	1.9204	0.9684	1.9206	0.9688
1/64	0.0045	1.9951	0.0065	1.9739	0.9654	0.9922	0.9654	0.9923
1/128	0.0011	1.9988	0.0016	1.9935	0.4834	0.9981	0.4834	0.9981
$O(h^r)$, $r =$		1.8616		1.6994		0.8888		0.8892

Numerical Results for Comp Ex 4 with $k = 9$

Table: Comparison example 4 with $k = 9$ by WG

h	$\|\nabla_d e_h\|$	$\|e_0\|$	$\|e_b\|$	$\|\nabla_d u_h \nabla u\|$	$\|u_0 - u\|$	$\|e_0\|_\infty$
1/4	7.98e+00	6.80e-02	2.93e-01	1.58e+01	2.52e-01	1.49e-01
1/8	3.89e+00	2.07e-02	7.44e-02	8.18e+00	1.30e-01	4.22e-02
1/16	1.91e+00	5.43e-03	1.88e-02	4.12e+00	6.53e-02	1.09e-02
1/32	9.54e-01	1.37e-03	4.72e-03	2.06e+00	3.27e-02	2.74e-03
1/64	4.76e-01	3.44e-04	1.18e-03	1.03e+00	1.63e-02	6.84e-04
$O(h^r)$, $r =$	1.0161	1.9160	1.9897	0.9857	0.9883	1.9492

Table: Comparison example 4 with $k = 9$ by SG

$h_{\mathcal{M}} := n^{-1}$	$\|e_u\|_\infty$	order	$\|e_u\|_{L^2(\Omega)}$	order	$\|e_u\|_{H^1(\Omega)}$	order	$\|e_u\|_{H^1(\Omega)}$	order
1/4	1.5663		0.4770		28.1833		28.1873	
1/8	0.7947	0.9788	0.4986	-0.0638	28.2982	-0.0059	28.3026	-0.0059
1/16	0.4728	0.7492	0.4292	0.2163	25.0052	0.1785	25.0089	0.1785
1/32	0.1341	1.8185	0.1738	1.3042	14.3673	0.7994	14.3683	0.7995
1/64	0.0339	1.9850	0.0489	1.8285	7.3446	0.9680	7.3448	0.9681
1/128	0.0085	1.9975	0.0126	1.9577	3.6889	0.9935	3.6890	0.9935
$O(h^r)$, $r =$		1.5177		1.0733		0.6087		0.6088

Observation

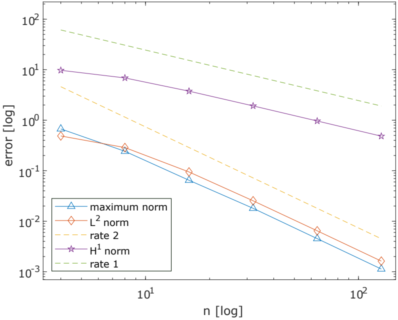

Figure: Comp Ex 4 with $k = 3$ by SG

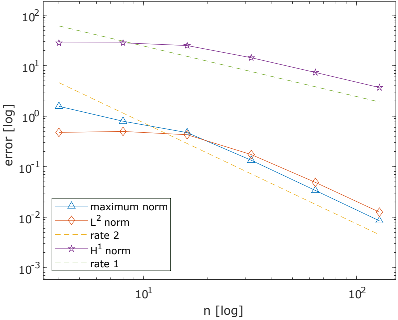

Figure: Comp Ex 4 with $k = 9$ by SG

From these results in Comp Ex 4 we can see that the SG attains its expected convergent orders (optimal convergence rates) in a rather slow pace compared to the WG.

Thankya!